12-1-2008

A Membrane-Type Humidifier for Fuel Cell Applications: Controller Design, Analysis and Implementation

Denise A. McKay
University of Michigan, Ann Arbor, dmckahn@smith.edu

Anna G. Stefanopoulou
University of Michigan, Ann Arbor

Jeffrey Cook
University of Michigan, Ann Arbor

Proceedings of FuelCell2008
Sixth International Fuel Cell Science, Engineering and Technology Conference
June 16-18, 2008, Denver, Colorado, USA

FuelCell2008-65257

A MEMBRANE-TYPE HUMIDIFIER FOR FUEL CELL APPLICATIONS: CONTROLLER DESIGN, ANALYSIS AND IMPLEMENTATION

Denise A. McKay, Anna G. Stefanopoulou, and Jeffrey Cook
Fuel Cell Control Laboratory*, University of Michigan, Ann Arbor, Michigan, 48109
Contact e-mail: dmckay@umich.edu

ABSTRACT

A membrane-based gas humidification apparatus was employed to actively manage the water vapor entrained in the reactant gas supplied to a fuel cell stack. The humidification system utilizes a gas bypass and a series of heaters to achieve accurate and fast humidity and temperature control. A change in fuel cell load induces a reactant mass flow rate disturbance to this humidification system. If not well regulated, this disturbance creates undesirable condensation and evaporation dynamics, both to the humidification system and the fuel cell stack. Therefore, controllers were devised, tuned and employed for temperature reference tracking and disturbance rejection. The coordination of the heaters and the bypass valve is challenging during fast transients due to the different time scales, the actuator constraints, and the sensor responsiveness. Two heater controller types were explored: on-off (thermostatic) and variable (proportional integral), to examine the ability of the feedback system to achieve the control objectives with minimal hardware and software complexity. This controller tuning methodology is useful for optimizing response time versus heater parasitic losses.

1 INTRODUCTION

For the advancement of polymer electrolyte membrane fuel cell (PEMFC) systems, achieving adequate thermal and humidity regulation remains a critical hurdle [1]. To maintain high membrane conductivity and durability, the supplied reactants require humidification. However, excess water can condense and affect fuel cell performance [2], requiring accurate and fast control of the gas humidity supplied to the fuel cell [3].

Several humidification strategies have been considered for fuel cell reactant pre-treatment, including bubblers or spargers [4], and passive membrane-based humidifiers integral to the PEMFC stack [2,5,6]. For active humidity and temperature control of the reactants supplied to a PEMFC stack, a stand-alone membrane-based humidification system was designed and experimentally validated [7]. The humidification apparatus decouples the passive membrane humidifier from the PEMFC cooling loops with the addition of an external gas bypass and a separate water circulation system, (PEMFC reactant exhaust streams could also be used), to provide a controllable reactant relative humidity at a regulated temperature. This humidification system apparatus is conceptually similar to that proposed by [8]. The operation of the humidifier consists of a dry reactant gas and liquid water delivered to opposite sides of a membrane humidifier to produce a saturated gas. Another stream of dry reactant gas bypasses the humidifier. The combination of the saturated and dry gas streams produces a reactant-vapor mixture at a desired relative humidity. A diagram of the humidification system is provided in Figure 1.

The humidification system control strategy in [8] relied on a relative humidity sensor for feedback control of an electronic bypass valve. Due to the strong coupling between gas humidity and temperature, thermal regulation must also be considered. We are unaware of any achievement claiming active con-

*Funding is provided by the U.S. Army Center of Excellence for Automotive Research (DAAE07-98-3-0022) and the National Science Foundation (CMS 0625610).

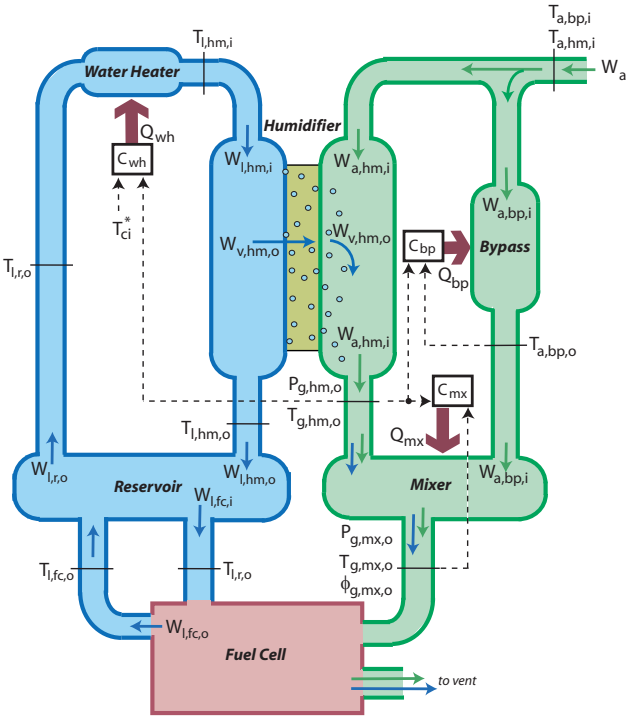

Figure 1. Overview of the control architecture for the external humidification system. Dashed lines indicate controller, C, input temperatures.

trol of the reactant humidity and cathode inlet temperature using a membrane-based humidification system suitable for automotive applications. In developing our control strategy, critical steps were accomplished by properly selecting the controller references used for temperature feedback; employing a static feedforward mapping for humidity control to eliminate the need for an expensive and slow relative humidity probe for feedback control; and providing a thorough comparison of the use of on/off versus variable gas heaters in achieving thermal regulation.

Controllers were designed and a reproducible methodology for controller tuning is presented to coordinate the three resistive heaters as well as the mass fractional split of air flow between the humidifier and air bypass. These controllers must regulate the temperature of the dry air leaving the bypass and joining the saturated air leaving the humidifier. Should the temperatures of these two gas streams not be well regulated during air mass flow disturbances due to the fuel cell system load demand, condensation or dehydration will occur. Similar problems arise in engine thermal management systems employing either a valve or servo motor to bypass coolant around the heat exchanger [9, 10]. The coordination of these heaters and the bypass valve is challenging during fast transients due to the different time scales, the actuator constraints, and the sensor responsiveness.

2 HUMIDIFICATION SYSTEM OVERVIEW

The humidification system hardware[1] was installed in the Fuel Cell Control Laboratory at the University of Michigan. The system was designed to deliver moist air to the cathode of a 500W fuel cell stack between 45^o-65^o C and 50%-100% relative humidity at dry air mass flow rates between 0-40 slm.

The humidifier system consists of five control volumes, namely the water heater, humidifier, reservoir, bypass, and mixer, shown in Fig. 1. For nomenclature, the letter M in (kg/mol) is used to denote molar mass, P in (Pa) for pressure, Q in (W) for heat added to a control volume, r for the fraction of the total air flow, T in (K) for temperature, W in (kg/s) for mass flow rate, and the symbol ϕ for relative humidity. Subscripts are used to indicate first the substance of interest, where a is for air, b for bulk materials, g for gas mixture, l for liquid water and v for water vapor; secondly the control volume such as bp for bypass, ca for cathode, cv generically for control volume, r for reservoir, fc for fuel cell, wh for water heater, hm for humidifier, and mx for mixer; finally an i or o indicates the control volume inlet or outlet. Superscripts are used as sat for saturation, o for nominal values, and $*$ for desired values.

When coupled with a fuel cell, the total dry air mass flow through the humidification system, W_a, depends on the amount of current produced by the fuel cell and is a system disturbance. The fraction of air supplied to the bypass, r_{bp}, or humidifier, r_{hm}, is controlled with mass flow controllers that regulate the bypass and humidifier air mass flow rates, $W_{a,bp,i}$, and $W_{a,hm,i}$. The humidifier produces a saturated air stream at a temperature, $T_{g,hm,o}$, dependent upon the supplied liquid water temperature, $T_{l,hm,i}$. Air bypassing the humidifier is heated with a 50W heater, Q_{bp}. The saturated air stream from the humidifier and dry air stream from the bypass are combined in the mixer to produce a desired air-vapor mixture relative humidity, $\phi_{g,mx,o}$, to be supplied to the fuel cell. A 52W resistive heater, Q_{mx}, is used in the mixer for temperature control and to minimize condensation during the mixing of the saturated and dry gases.

Liquid water is circulated from the reservoir through the water heater and humidifier using a pump and manual throttle valve. The reservoir is shared with the fuel cell coolant, shown with an input to the reservoir at the fuel cell coolant temperature, $T_{l,fc,o}$. The humidification system is designed to heat the supplied reactants to the temperature of the coolant leaving the fuel cell stack. If the water system is well insulated and well controlled, the waste heat from the fuel cell stack is used to maintain the water reservoir temperature. However, a 1000W resistive heater, Q_{wh}, is used to heat the liquid water before entering the humidifier to mitigate thermal disturbances and offset heat losses to the ambient. Note, this water heater power should be chosen based on the fuel cell electrical subsystem design to ensure that the heater is supported during thermal transients.

[1]Designed in collaboration with the Schatz Energy Research Center at Humboldt State University

3 MODELING SUMMARY

This section summarizes the humidification system modeling effort that was experimentally validated in [7]. Applying the conservation of mass and energy, the resulting state equations are expressed for the bypass,

$$\frac{dT_{a,bp}}{dt} = \frac{1}{m_{bp}C_{bp}}\left[Q_{bp} + W_{a,bp,i}C_{p,a}(T_{a,bp,i} - T_{a,bp,o}) - \bar{h}_{b2amb,bp}A_{b2amb,bp}(T_{a,bp} - T_{amb})\right], \quad (1)$$

the water reservoir,

$$\frac{dT_{l,r}}{dt} = \frac{1}{m_{l,r}C_{l,r}}\left[W_{l,fc,i}C_{p,l}(T_{l,fc,o} - T_{l,r,o}) + W_{l,wh,i}C_{p,l}(T_{l,hm,o} - T_{l,r,o}) - \bar{h}_{l2b,r}A_{l2b,r}(T_{l,r} - T_{b,r})\right], \quad (2a)$$

$$\frac{dT_{b,r}}{dt} = \frac{1}{m_{b,r}C_{b,r}}\left[\bar{h}_{l2b,r}A_{l2b,r}(T_{l,r} - T_{b,r}) - \bar{h}_{b2amb,r}A_{b2amb,r}(T_{b,r} - T_{amb})\right], \quad (2b)$$

the water heater,

$$\frac{dT_{l,wh}}{dt} = \frac{1}{m_{l,wh}C_{l,wh}}\left[W_{l,hm,i}C_{p,l}(T_{l,r,o} - T_{l,hm,i}) + \bar{h}_{b2l,wh}A_{b2l,wh}(T_{b,wh} - T_{l,wh})\right], \quad (3a)$$

$$\frac{dT_{b,wh}}{dt} = \frac{1}{m_{b,wh}C_{b,wh}}\left[Q_{wh} - \bar{h}_{b2l,wh}A_{b2l,wh}(T_{b,wh} - T_{l,wh}) - \bar{h}_{b2amb,wh}A_{b2amb,wh}(T_{b,wh} - T_{amb})\right], \quad (3b)$$

the humidifier,

$$\frac{dT_{l,hm}}{dt} = \frac{1}{m_{l,hm}C_{l,hm}}\left[W_{l,hm,i}C_{p,l}(T_{l,hm,i} - T_{l,hm,o}) - \bar{h}_{l2g,hm}A_{l2g,hm}(T_{l,hm} - T_{g,hm}) - W_{v,hm,o}C_{p,v}T_{g,hm,o} - \bar{h}_{l2amb,hm}A_{l2amb,hm}(T_{l,hm} - T_{amb})\right], \quad (4a)$$

$$\frac{dT_{g,hm}}{dt} = \frac{1}{m_{g,hm}C_{g,hm}}\left[W_{a,hm,i}C_{p,a}(T_{a,hm,i} - T_{g,hm,o}) + \bar{h}_{l2g,hm}A_{l2g,hm}(T_{l,hm} - T_{g,hm})\right], \quad (4b)$$

and the mixer,

$$\frac{dT_{g,mx}}{dt} = \frac{1}{m_{g,mx}C_{g,mx}}\left[W_{a,bp,i}C_{p,a}(T_{a,bp,o} - T_{g,mx,o}) + (W_{a,hm,i}C_{p,a} + W_{v,hm,o}C_{p,v})(T_{g,hm,o} - T_{g,mx,o}) + \bar{h}_{b2g,mx}A_{b2g,mx}(T_{b,mx} - T_{g,mx})\right], \quad (5a)$$

$$\frac{dT_{b,mx}}{dt} = \frac{1}{m_{b,mx}C_{b,mx}}\left[Q_{mx} - \bar{h}_{b2g,mx}A_{b2g,mx}(T_{b,mx} - T_{g,mx}) - \bar{h}_{b2amb,mx}A_{b2amb,mx}(T_{b,mx} - T_{amb})\right]. \quad (5b)$$

A list of the parameter values was given in [7]. The relative humidity of the mixer outlet gas is estimated by

$$\phi_{g,mx,o} = \phi_{g,hm,o}\, r_{hm}\, \frac{p^{sat}_{g,hm,o}}{p^{sat}_{g,mx,o}} \left(\frac{p_{g,mx,o}}{p_{g,hm,o} - r_{bp}\, \phi_{g,hm,o}\, p^{sat}_{g,hm,o}}\right). \quad (6)$$

Due to the inability to measure the internal temperature states, approximations were employed to relate the internal states to the measurable outlet temperatures and are summarized by

$$T_{a,bp,o} = 2T_{bp} - T_{a,bp,i}, \quad (7a)$$
$$T_{l,wh,o} = 2T_{l,wh} - T_{l,r,o}, \quad (7b)$$
$$T_{l,hm,o} = 2T_{l,hm} - T_{l,hm,i}, \quad (7c)$$
$$T_{l,r,o} = T_{l,r}, \quad (7d)$$
$$T_{a,hm,o} = 2T_{a,hm} - T_{a,hm,i}, \quad (7e)$$
$$T_{g,mx} = T_{g,mx,o}. \quad (7f)$$

The locations of the measurements and disturbances are shown in Figure 1. The inputs to the system are heater power, Q, and the mass fraction of air diverted through the bypass, r_{bp}; the states are the respective temperatures, T; the disturbances are the total dry air mass flow rate, W_a, the air temperature supplied to the system, $T_{a,hm,i}$ and $T_{a,bp,i}$, and the ambient temperature, T_{amb}; and the system output is the air relative humidity leaving the mixer, $\phi_{g,mx,o}$.

4 CONTROLLER ARCHITECTURE

With the model of the external humidification system presented in Section 3, controllers were designed and tuned to coordinate the heaters as well as the fraction of air supplied to the humidifier and bypass. The three heaters must be well coordinated to regulate the system temperatures and mitigate the effect of disturbances. This section introduces the nonlinear static feedforward mapping devised for air mass flow control along with the reference temperatures used for thermal regulation.

4.1 Nonlinear Feedforward for Air Mass Flow Control

Direct relative humidity feedback control requires either a water vapor mass flow rate or relative humidity measurement at the mixer outlet. In practice, both measurements are prohibitively expensive. Although an observer based relative humidity feedback estimation could be employed, the coupling between humidity and temperature poses a performance tradeoff between these two control objectives, motivating the rationale for feedforward humidity regulation.

To calculate the desired split of dry air mass flow between the humidifier and the bypass, mass conservation is applied. Assuming that in steady-state the mass flow rate of water vapor and air entering the mixer are equal to the mass flow rates leaving the mixer, and applying the definition for the humidity ratio, $\omega = \frac{M_v \phi p^{sat}}{M_a(p - \phi p^{sat})}$, the required fraction of air supplied to the hu-

midifier, $r_h = W_{a,hm,i}/W_a$, can be expressed as

$$r_{hm} = \frac{\phi^*_{g,mx,o} p^{sat*}_{g,mx,o} (p_{g,hm,o} - \phi_{g,hm,o} p^{sat}_{g,hm,o})}{\phi_{g,hm,o} p^{sat}_{g,hm,o} (p_{g,mx,o} - \phi^*_{g,mx,o} p^{sat*}_{g,mx,o})} \quad (8)$$

where a superscript $*$ has been used to denote desired reference values. The commanded air mass flow rates through the humidifier and the bypass are:

$$W_{a,hm,i} = r_{hm} W_a, \quad (9a)$$

$$W_{a,bp,i} = W_a - W_{a,hm,i}. \quad (9b)$$

4.2 Reference Temperatures

To properly coordinate the heaters using feedback control, reference temperatures must be established for the mixer, bypass and humidifier air outlets. The error, or difference between the reference and actual measured temperatures, $\delta e = \delta T^* - \delta T$ where δ indicates a deviation from nominal conditions, can then be formulated into control objectives for each of the heaters.

Several reference temperature choices exist for thermal regulation of the humidification system, depending upon the response times of the bypass, mixer and water circulation systems. These reference temperatures have drastically different implications with respect to controller performance. For example, if the water circulation, bypass and mixer systems had similar response times, they could be independently coordinated, motivating the selection of the desired cathode inlet temperature as the reference temperature for all three systems. It will be shown later, in Section 5, that the intermediate step of heating liquid water to raise the humidifier gas temperature causes the slowest thermal response of the three systems. Because both the mixer and bypass systems are faster than the water circulation system, condensation or evaporation can be avoided upon gas mixing if both the mixer and the bypass track the temperature dynamics of the water circulation system. The resulting reference temperatures,

$$T^*_{g,mx,o} = T_{g,hm,o}\ , \qquad T^*_{g,hm,o} = T^*_{ca,i}\ , \qquad T^*_{a,bp,o} = T_{g,hm,o}\ , \quad (10)$$

will result in a slower system thermal response but will maintain the desired relative humidity. Figure 1 shows the location of these reference temperatures with the measured states and respective control volumes clearly indicated.

5 PLANT LINEARIZATION AND POLE SENSITIVITY

The system of ordinary differential equations, shown in Section 3, was expressed analytically in state space where the control volume outlet temperatures represented the states, the heater actuators represented the system inputs, the air mass flow rate represented the system disturbance, and the liquid water mass flow rate and ambient temperature were assumed to be constant. Using this state space representation, the system was linearized about a set of nominal conditions where W^o_a=0.6 g/s, r^o_h=0.7, $T^o_{a,hm,i}$=$T^o_{a,bp,i}$=20^{o}C, $W^o_{l,hm,i}$=30 g/s, T^o_{amb}=27^{o}C, $p^o_{g,hm,o}$=102.57 kPa abs, and $T^o_{a,bp,o}$=$T^o_{g,hm,o}$=55^{o}C. As previously discussed, the humidification system was designed to regulate the cathode air supplied to an 8-cell PEMFC stack with an active area of 300cm^2. Applying a 0.3A/cm^2 electric load to this PEMFC stack requires 0.6 g/s of air at an air stoichiometry of 250%. These nominal conditions were selected to approximate the midpoint of the expected stack operating range.

Transfer functions from the heater inputs to the outlet temperatures were then derived and the sensitivity of the pole locations on total air mass flow rate was examined. Table 1 summarizes the open loop time constants and DC-gains for this range of air flow for each of the three systems. The total air mass flow rate range considered, W_a=0.3-0.9 g/s, represents a humidification system disturbance for PEMFC stack electrical loads between 0.15-0.45A/cm^2. The linear and nonlinear systems were compared, both to steps in heater inputs and air mass flow rates, indicating that the linear system response well approximates the nonlinear system for small deviations from nominal conditions.

Table 1. Open loop characteristics for W_a=0.3-0.9 g/s.

System	**DC-gain**(^{o}C/W) $\frac{\delta T_{g,cv,o}}{\delta Q_{cv}}\big\vert_{s=0}$	**Time Constant**(sec)
Water Circulation	0.10-0.08	123-59
Bypass	6.93-3.32	1490-1195
Mixer	1.01-0.52	714-498

Transfer functions can also be expressed from the air flow disturbance to the outlet temperatures. However, the DC gains of these transfer functions indicate that there is a very small change in the steady-state heat required for a change in air mass flow rate. As a result, the use of static feedforward to reject air flow disturbances does not significantly improve temperature regulation. Therefore, only transfer functions from the heater inputs to the temperature outputs will be presented here.

The first order analytical transfer function from the bypass heater input to the bypass air outlet temperature, assuming the dry air mass flow rate is constant, is expressed as

$$\frac{\delta T_{a,bp,o}}{\delta Q_{bp}} = \frac{b_{0,bp}}{s + p_{bp}}\ , \quad (11)$$

where the numerator coefficient and pole location are defined by

$$b_{0,bp} = \frac{2}{m_{bp} C_{bp}}\ ,$$

$$p_{bp} = \frac{2W^o_{a,bp,i} C_{p,a} + \bar{h}^o_{b2amb,bp} A_{b2amb,bp}}{m_{bp} C_{bp}} \approx 0.013\ .$$

The bypass pole location (denoted by p_{bp}) is a function of the air mass flow rate through the bypass which will influence the system response time and DC-Gain as indicated in Table 1.

A transfer function from the water heater actuator input to

the humidifier air outlet temperature is expressed as

$$\frac{\delta T_{g,hm,o}}{\delta Q_{hm}} = \frac{b_0(s+z_1)}{(s+p_{l,wh})(s+p_{l,hm})(s+p_{a,hm})(s+p_{l,r})(s+p_{b,r})}, \quad (12)$$

where the coefficient in the numerator, b_0, and the pole and zero locations can be analytically represented as functions of the heat transfer coefficients and the control volume masses and specific heats. At the nominal conditions, b_0=3.38x10^{-6} and the poles and zero are located at $p_{a,hm}$=1.23, $p_{l,hm}$=0.292, $p_{l,r}$=0.090, $p_{b,r}$=8.2x10^{-4}, $p_{l,wh}$=0.014, and z_2=0.0094, with a pole-zero cancelation between z=$p_{b,wh}$=0.016. The fastest control volume response time (pole location furthest from the origin on the complex s-plane) is the humidifier air, followed by the liquid water volumes, with the bulk volumes having the slowest response time. As with the bypass, the water circulation system response time increases for increasing air mass flow rates.

The mixer thermal dynamics are described by a two state system including the air-vapor mixture and the bulk materials. At the nominal conditions, the pole associated with the gas state is located at s=-0.132 while the pole associated with the bulk materials is located at s=-0.0017, indicating a significant bandwidth separation between these two states. As a result, assuming that $\frac{\delta T_{g,mx,o}}{dt}$=0, a first order analytical transfer function from the mixer heater input to the gas outlet temperature, is expressed by

$$\frac{\delta T_{g,mx,o}}{\delta Q_{mx}} = \frac{b_{0,mx}}{s+p_{mx}} \quad (13)$$

where,

$$\begin{aligned}
b_{0,mx} &= \bar{h}^o_{b2g,mx} A_{b2g,mx} / \beta_{3,mx}, \\
\beta_{1,mx} &= \bar{h}_{b2amb,mx} A_{mx} + \bar{h}^o_{b2g,mx} A_{b2g,mx}, \\
\beta_{2,mx} &= \left(W^o_a C_{p,a} + W^o_{v,hm,o} C_{p,v}\right), \\
\beta_{3,mx} &= m_{b,mx} C_{b,mx} \left(\beta_{2,mx} + \bar{h}^o_{b2g,mx} A_{b2g,mx}\right), \\
p_{mx} &= \frac{\beta_{1,mx}\beta_{2,mx} + \bar{h}_{b2amb,mx} A_{mx} \bar{h}^o_{b2g,mx} A_{b2g,mx}}{\beta_{3,mx}}.
\end{aligned}$$

Comparing the nonlinear full order model to this linear reduced order model of the mixer thermal dynamics during step changes in mixer heat shows an insignificant difference between the two dynamic models. Clearly, the mixer pole location is a function of the air mass flow rate, either directly, or indirectly through the heat transfer coefficient (between the bulk materials and the gases) or the water vapor mass flow rate. As expected, by comparing the DC-Gains of the bypass and mixer, more energy is required to raise the mixer temperature due to the larger air mass and the presence of water vapor in the mixer.

6 Thermostatic Control

A widely used, simple and inexpensive control strategy employs thermostatic (two position or on-off) control to cycle a heater. A commonly recognized disadvantage to thermostatic control is the cycling of the actuator due to the repeated on-off action resulting from sensor noise. To reduce this cycling, hysteresis is often incorporated to construct a region about the desired temperature for which no control action takes place.

When the temperature error, $e = T^* - T$, is less than the lower error bound, $e < -e_s$, the heater is on ($Q = Q_{max}$). When the temperature error is greater than the higher error bound $e > e_s$, the heater is off ($Q = 0$). For errors within the error bounds, there is hysteresis such that the heater is either on or off depending upon the previous state of the heater. In summary, the discrete time thermostatic control law is represented by,

$$u(k) = \begin{cases} Q_{max}, & \text{for } e(k) \le -e_s, \\ 0, & \text{for } e_s \le e(k), \\ u(k-1), & \text{for } -e_s < e(k) < e_s. \end{cases} \quad (14)$$

Some degree of temperature overshoot, $|e| > |e_s|$, is expected after the heater turns on or off; thus, the steady temperature response is oscillatory. The frequency and magnitude of these induced limit cycle oscillations will depend on the system thermal dynamics and the error bounds, e_s, at which the heater is switched on or off. The error bound will be selected to keep the error, e, within a specified limit cycle amplitude, a.

Selecting this error bound, e_s, is not trivial. Both a describing function methodology as well as a simulation based strategy were employed to tune the thermostatic controllers for the three resistive heaters, as detailed in the following subsections. Table 2 shows the amplitude and, where applicable, the limit cycle period for each of the three regulated systems evaluated at the nominal conditions.

Table 2. Summary of thermostatic control results.

System	Error Bound	Amplitude	Period
Bypass	0.38^{o}C	0.5^{o}C	2 sec
Mixer	0.38^{o}C	1.0^{o}C	n/a
Water Circulation	0.21^{o}C	0.5^{o}C	58 sec

6.1 Water Circulation System Tuning with Describing Function Method

Describing functions have been used to quantify the amplitude and frequency of limit cycles induced in relay feedback systems [11, 12], and subsequently used in the tuning of process controllers [13]. A describing function that approximates the behavior of an ideal relay with hysteresis ($u = \pm Q_{max}$) was derived in [14]. The physical heater actuators employed, however, do not allow negative heat to be added to the control volume. As a result, the describing function in [14] was shifted and scaled, resulting in

$$N(a^*, e_s) = \frac{Q_{max}}{2}\left[\frac{4}{\pi a^*}\left(\sqrt{1-\left(\frac{e_s}{a^*}\right)^2} - j\frac{e_s}{a^*}\right) + 1\right], \quad (15)$$

where a^* is the desired temperature limit cycle amplitude.

In a relay feedback system, the output temperature of the thermal process, $\delta T(s) = G(s)\delta Q(s)$ where $G(s)$ denotes the plant transfer function (shown in Section 5), oscillates with a temperature amplitude of a and frequency ω. Assuming there is no change in the reference temperature and no disturbances to the system, the error bound and the resulting frequency of oscillation can be determined for a given desired amplitude by satisfying both the real and imaginary parts of $G(j\omega)N(a^*, e_s) = -1 + 0j$. As the differential gap expands, the resulting limit cycle oscillation amplitude increases and the frequency decreases.

If the desired limit cycle oscillation is not known, it can be calculated using the following steps based on a combination of the smallest achievable output amplitude, a_{ideal}, (which occurs for an ideal relay with no hysteresis), and the temperature measurement noise.

1) A describing function for a shifted ideal relay is formulated by setting e_s=0 in Equation 15.
1) The resulting output amplitude which corresponds to the smallest achievable amplitude, a_{ideal}, is calculated by solving $G(j\omega)N(a^* = a_{ideal}, e_s = 0) = -1 + 0j$.
2) The standard deviation in the measurement output noise, σ_n, is quantified.
3) A combination of the smallest achievable output amplitude and the measurement noise is constructed, such as $a^* = a_{ideal} + 3\sigma_n$.

The smallest achievable humidifier air outlet temperature oscillations are $a_{ideal,wh} \approx 0.2^oC$. As a result, the desired output amplitude for the water circulation system is $a^*_{wc} \approx 0.5^oC$. From evaluation of $\frac{\delta T_{g,hm,o}}{\delta Q_{wh}}(j\omega)N(a^*_{wc}, e_{s,wc}) = -1 + 0j$, the resulting error bound is $e_{s,wc} \approx 0.2^oC$ which induces a limit cycle of frequency $\omega_{wc} \approx 0.11$ rad/s (corresponding to an oscillation period of 58 seconds).

6.2 Bypass and Mixer Tuning by Simulation

For first order plants, the describing function methodology cannot be employed to analytically calculate the thermostatic error bounds. The Nyquist plot of a first order plant remains in the right hand plane. Thus, no intersection exists between the describing function, which accounts for the fundamental component of the nonlinear relay element, and the plant Nyquist. Instead, simulations of the non-ideal relay feedback system are used to examine the resulting temperature limit cycles for the bypass and mixer systems.

To tune the thermostatic error bounds using a simulation based approach, first the error bound is set equal to the desired amplitude of the output temperature oscillations. The error bound is then incrementally reduced until the simulated temperature error is less than the desired amplitude. This process is summarized as follows.

1) The desired output amplitude, a^*, is selected.
2) The initial temperature error bounds are chosen to be equal to the desired temperature output amplitude, such that e_s=a^*.
3) The closed loop non-ideal relay feedback system response is simulated using the nonlinear plant model evaluated at the nominal operating conditions.
4) The simulated temperature error signal is compared to the desired amplitude.
5) If the simulated temperature error remains smaller than the desired amplitude throughout the simulation, then the search is terminated. Otherwise, the temperature error bounds are reduced and steps 3-5 are repeated.

Of course, in the physical system, the thermostatically controlled water heater will induce humidifier gas outlet temperature oscillations that influence both the bypass and the mixer, as inputs and/or dynamic reference temperatures. Therefore, it is recommended that the bypass and mixer thermostatic controllers be tuned in a manner that accounts for the water circulation system performance. By first selecting the water heater error bounds, as discussed in Section 6.1, the error bounds for the bypass relay feedback system can be determined using the simulation based iterative approach described above. Then given the error bounds for the bypass and water heater, the error bounds for the mixer relay feedback system can be determined via simulation.

In selecting the desired amplitudes for the bypass and mixer, consideration of the system dynamics must be made. As with the water heater, the desired bypass temperature limit cycle amplitude was selected to be a^*_{bp}=0.5^oC. Because the mixer receives air and water vapor from the humidifier, oscillations in the humidifier will cause oscillations in the mixer even when the mixer heater is off. As a result, the mixer amplitude was selected to be a^*_{mx}=1.0^oC to account for the 0.5^oC amplitude fluctuations due to the water circulation system.

Applying this iterative and sequential simulation based tuning approach, at the nominal operating conditions, the bypass error bound was found to be $e_{s,bp}$=0.38^oC to achieve a temperature limit cycle amplitude of a^*_{bp}=0.5^oC and the mixer error bound was $e_{s,mx}$=0.38^oC to achieve a temperature limit cycle amplitude of a^*_{bp}=1.0^oC. Although the error bounds for the bypass and mixer are the same, the two systems produce different temperature limit cycle amplitudes.

7 PROPORTIONAL INTEGRAL CONTROL

The thermostatic controllers, designed in Section 6, are inexpensive to implement and are capable of regulating temperature to within 1^oC of the desired cathode inlet temperature. If, however, zero steady-state temperature error is required or the limit cycle temperature oscillations are undesirable, a more sophisticated controller is needed. With the addition of controller integrator states, zero steady-state error to a step command in the reference temperature can be achieved. As a result, proportional integral (PI) control was considered due to the simplicity

of tuning with time domain constraints and guarantee of zero steady state error. Note, however, that in contrast to thermostatic control, PI control requires the heater actuators to be capable of producing a variable heat transfer rate. Thus, there is a tradeoff between regulation capability and hardware and software complexity.

The PI controller is expressed in the frequency domain as

$$\delta Q = \left(k_{P,cv} + \frac{k_{I,cv}}{s} \right) e \, , \tag{16}$$

where the proportional and integral controller gains are denoted by $k_{P,cv}$ and $k_{I,cv}$, respectively, for each control volume. By substitution into Equations 11 and 13, the mixer and bypass closed loop transfer functions from the reference to the actual temperature is described by,

$$\frac{\delta T_{g,cv,o}}{\delta T^*} = \frac{b_{o,cv} k_{P,cv} (s + k_{I,cv}/k_{P,cv})}{s^2 + (b_{o,cv} k_{P,bp} + p_{cv}) s + b_{o,cv} k_{I,bp}} \tag{17}$$

where p_{cv} is the open loop pole location. The PI controller gains can be tuned upon inspection of the characteristic polynomial of this closed loop transfer function. For tuning the controller gains, two of the following three time domain constraints are selected, from 1) the proportional controller gain, 2) response time, and 3) the damping coefficient (overshoot).

The mixer and bypass proportional gains are selected based on the expected maximal actuator heater power (at steady-state over the range of operating conditions) supplied, $Q_{design,cv}$, for a specified temperature error, $e_{design,cv}$, such that

$$k_{P,cv} = \frac{Q_{design,cv}}{e_{design,cv}} \, . \tag{18}$$

Given an expected error of $e_{design,cv}$=1.0K (corresponding to a^*=0.5K used for thermostatic controller tuning) and the maximum steady-state heater power of $Q_{design,bp}$=15W and $Q_{design,mx}$=25W, the proportional gains are $k_{P,bp}$=15W/K, $k_{P,mx}$=25W/K. For a critically damped response, the resulting integral controller gains can then be calculated. Note, if the heater power were reduced due to limitations of the electrical subsystem, the closed loop thermal response time would increase accordingly.

The closed loop transfer function from the desired humidifier air outlet temperature to the actual temperature is sixth order; therefore, time domain design constraints (overshoot, settling time, etc.) cannot be used analytically to specify the controller gains. Instead, iterative pole placement was used to achieve a desired closed loop response. From inspection of the open loop water circulation system poles and zeros, a stable slow pole is located on the real axis at approximately s=-0.0008. This pole could be shifted or canceled by a carefully tuned PI controller. Because the humidifier water circulation system has an air flow input disturbance and the model parameters were well identified, a pole shifting controller was employed for improved input disturbance rejection [15]. Using the linearized model of the water circulation system, shown in Equation 12, the PI controller was tuned to achieve a fast response with less than 20% overshoot.

A summary of the final controller gains and resulting settling times to a step in the reference temperature is shown in Table 3, along with the gain and phase margins. To prevent integrator windup, a logic based case structure was employed which enables or disables the integrator while the actuator is saturated at $Q_{cv}(t)$ =0 or $Q_{cv}(t) = Q_{max,cv}$.

Table 3. Proportional-integral controller gains and system response

Heater	$k_{P,cv}$	$k_{I,cv}$	t_{settle} (s)	GM (dB)	PM (deg)
Bypass	15	3.25	9.4	∞	142
Mixer	25	0.22	256	∞	145
Water Heater	263	1.60	176	20	138

8 CONTROLLER PERFORMANCE COMPARISON

To compare the thermostatic and PI controller responses for a step in the cathode inlet reference temperature from nominal conditions, a closed loop experiment was conducted, as shown in Figures 2-5. It is important to note that the fuel cell stack is not connected to the water reservoir during these experiments, thus waste heat from the fuel cell is not being used to maintain the reservoir water temperature. As a result, significantly more energy is required to heat the liquid water supplied to the fuel cell stack than would be expected during normal operation.

Using thermostatic control, the desired 0.5^{o}C humidifier air outlet temperature limit cycle amplitude was achieved, see Figure 2. Additionally, the time required to transition from the minimum to maximum limit cycle temperature, approximately 34 seconds, closely matched the expected value. Note, a 68 second period would have resulted if the free and forced response times were the same. For the water circulation system PI controller, the resulting overshoot following the step in the reference temperature is larger than predicted in simulation but still within the designed 20%.

The bypass responses to this reference step is shown in Figure 3. The resulting temperature limit cycle amplitude is approximately 0.5^{o}C, as designed. Throughout the experiment, the PI controller tracks the dynamic reference humidifier air outlet temperature with approximately zero steady-state error. The mixer responses to the temperature reference step is shown in Figure 4. The limit cycle amplitude was found to be slightly less than the designed 1^{o}C. The mixer PI controller performed as expected throughout the experiment. The mixer outlet relative humidity response for this temperature reference step is shown in Figure 5. Because the actual mixer outlet temperature response is approximately sinusoidal using thermostatic control, the relative humidity also exhibits an approximately sinusoidal response. Both

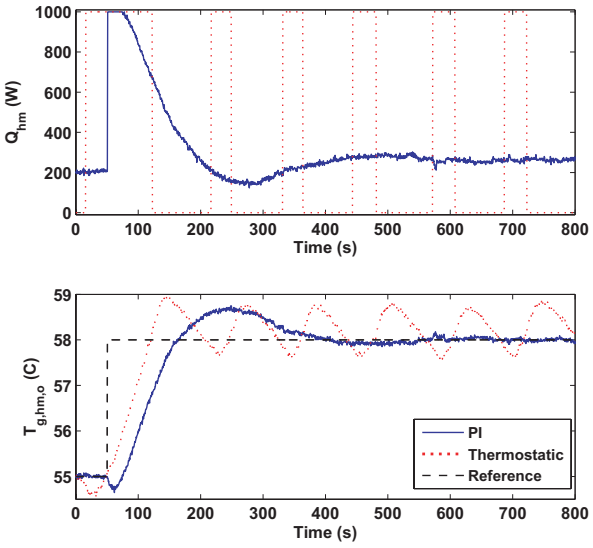

Figure 2. Experimental humidifier air outlet closed loop temperature response to a reference step, comparing PI and thermostatic control.

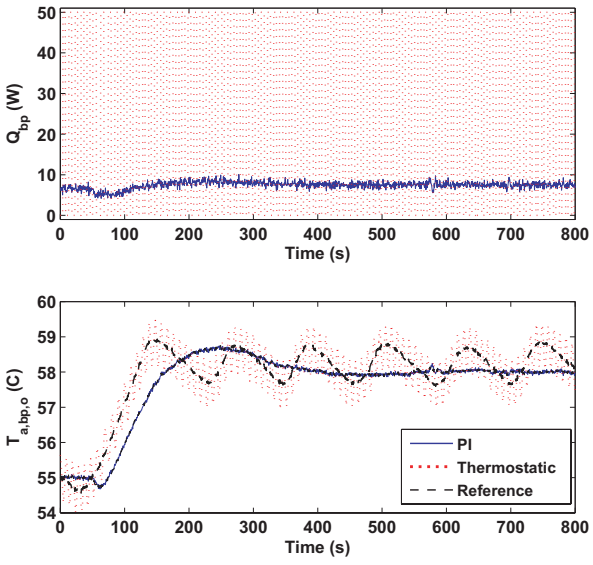

Figure 3. Experimental bypass air outlet closed loop temperature response to a reference step, comparing PI and thermostatic control.

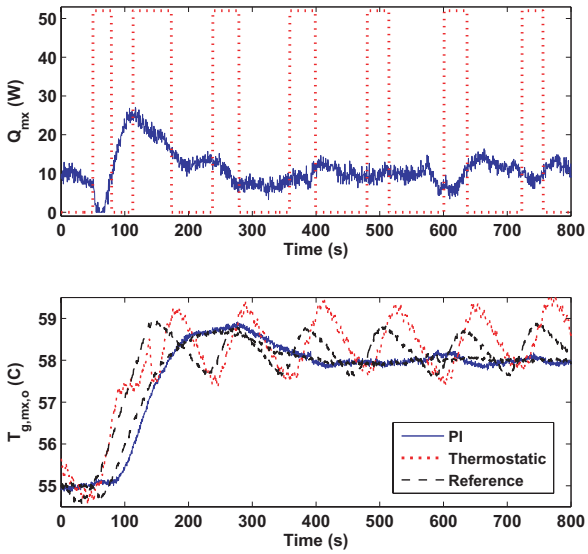

Figure 4. Experimental mixer air outlet closed loop temperature response to a reference step, comparing PI and thermostatic control.

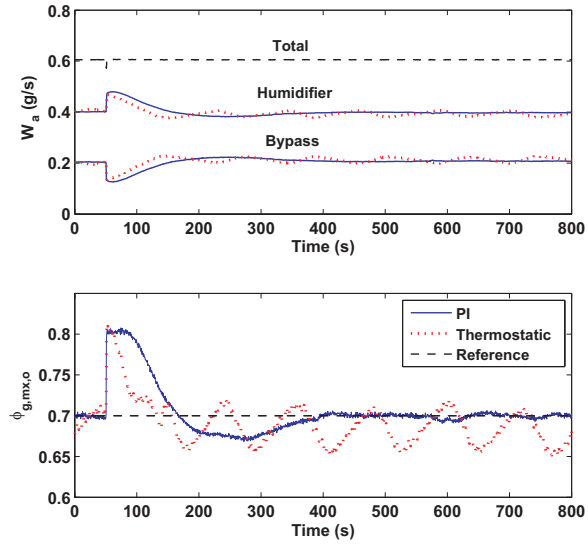

Figure 5. Mixer gas outlet relative humidity response to a step in the reference temperature, comparing PI and thermostatic control.

in simulation and in the experiment, the maximum excursion in the mixer air outlet relative humidity is approximately 10% for both controllers. Note, the mixer gas outlet relative humidity presented here is an estimation based on physical measurements applying Equation 6.

9 PI CLOSED LOOP DISTURBANCE RESPONSE

Using feedforward control of the air mass flow rate and proportional integral control of the resistive heaters, another closed loop experiment was conducted for changes in the system references (cathode inlet temperature and relative humidity) and the system disturbances (ambient temperature, total air mass flow, and a reservoir fill event). As expected the PI controller results in zero steady-state error. The overshoot and response time following step changes in reference temperature is approximately equal to the response the controller was tuned to achieve.

Figure 6 shows the humidifier air outlet temperature re-

sponse to disturbances. Interestingly, the cathode inlet reference temperature step results in an increase in the air flow supplied to the humidifier, causing an initial decrease in the humidifier air outlet temperature which resembles a non-minimum phase response but is actually due to the feedforward regulation of air flow. The rapid 10^oC increase in ambient temperature increased the humidifier air outlet temperature, requiring the humidifier heater power to decrease to regulate the air temperature. A decrease in total air flow resulted in a decrease in the fraction air supplied to the humidifier, in turn increasing the humidifier air outlet temperature. The reservoir fill event, which injects cold water into the reservoir, causes a dramatic decrease in the humidifier air outlet temperature that initially saturates the water heater. Finally, the decrease in desired cathode inlet relative humidity decreases the humidifier air flow in turn increasing the air outlet temperature.

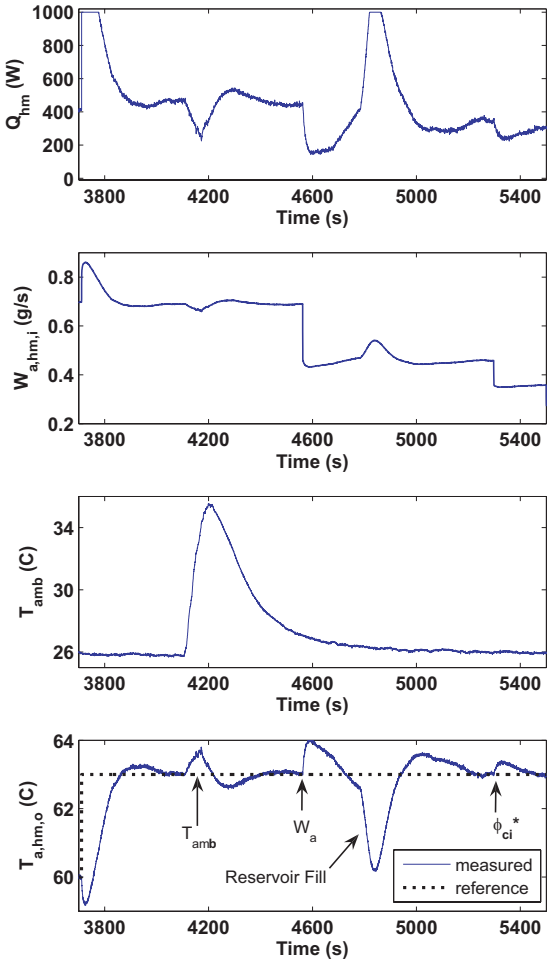

Figure 6. Humidifier air outlet response to disturbances using PI control.

The response of the bypass system to these disturbances is shown in Figure 7. Again, the intent of the bypass controller is to track the humidifier air outlet temperature. The bypass adequately tracks the humidifier air outlet temperature excursions well due to the difference in closed loop response times of these two systems. There is an insignificant difference between the bypass and humidifier air outlet temperatures throughout the experiment.

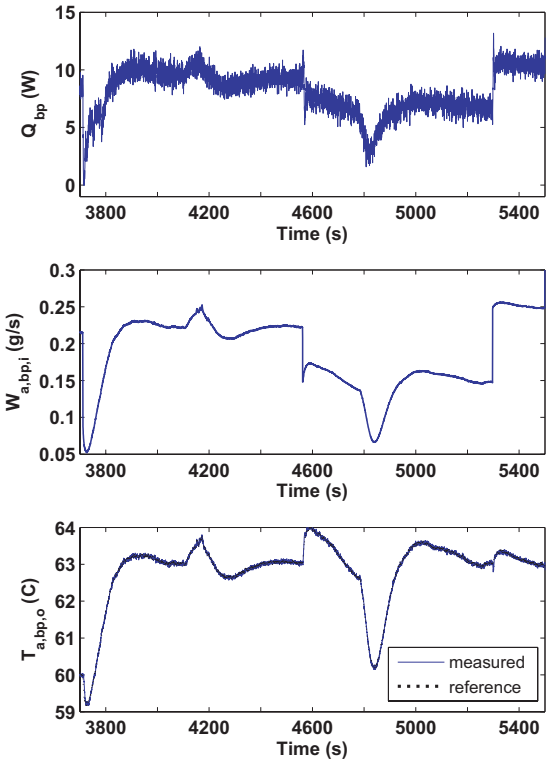

Figure 7. Bypass air outlet response to disturbances using PI control.

When the humidifier air outlet temperature initially decreases following the increase in the cathode inlet temperature reference, the mixer heater turns off and then proceeds to track the humidifier air outlet temperature, as shown in Figure 8. In general the ability of the mixer to track the humidifier is adequate. Additionally, the mixer outlet relative humidity is well regulated throughout the experiment. Although the relative humidity at the mixer outlet was relatively well regulated with thermostatic control, the temperature oscillations may not be desirable depending upon the operating conditions of the PEMFC stack to which the air is supplied. To eliminate these oscillations, proportional-integral (PI) control is recommended to guarantee zero steady-state temperature error. If variable heaters are available with no cost or reliability penalty with respect to control implementation, then the PI controllers are recommended.

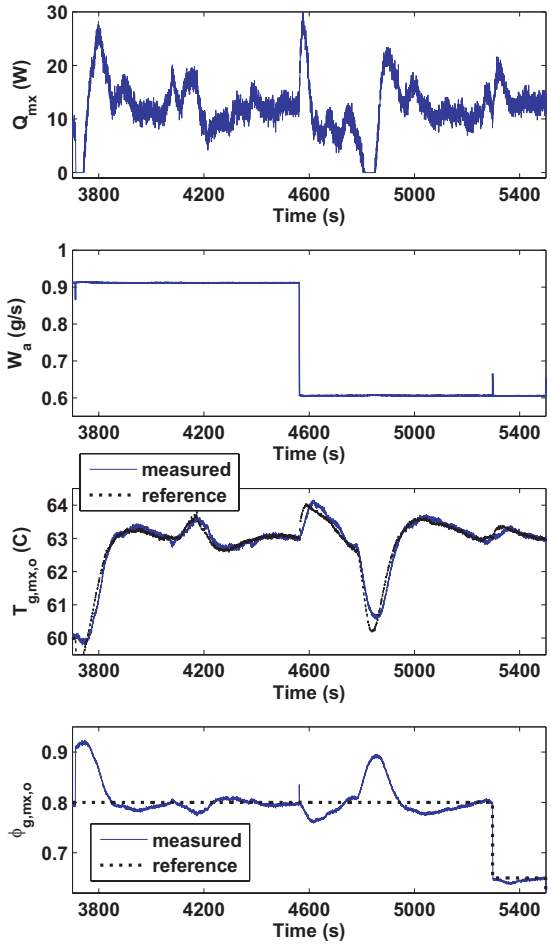

Figure 8. Mixer outlet response to disturbances using PI control.

10 CONCLUSIONS

An experimentally validated model of the humidification system thermal dynamics was employed to design and tune controllers for thermal and humidity regulation. Thermostatic and proportional-integral controllers were considered for thermal regulation, and a static nonlinear feedforward map was employed to control the air split between the humidifier and bypass. For constant disturbances, the humidification system dynamics are approximately linear enabling linear control theory to be applied for controller tuning. As expected, thermostatic control of the humidification system, tuned using either a describing function or simulation based methodology, resulted in temperature and relative humidity limit cycle oscillations. PI control, however, allowed for adequate control of both temperature and humidity with zero steady-state temperature error, while satisfactorily minimizing excursions in temperature following changes in the disturbances. Therefore, a tradeoff exists between steady-state thermal regulation and hardware and controller simplicity, a critical consideration for automotive applications.

REFERENCES

[1] Varigonda, S., and Kamat, M., 1996. "Control of stationary and transportation fuel cell systems: Progress and opportunities". *Computers and Chemical Engineering*, **30**, pp. 1735–1748.

[2] McKay, D., Siegel, J., Ott, W., and Stefanopoulou, A., 2008. "Parameterization and prediction of temporal fuel cell voltage behavior during flooding and drying conditions". *Journal of Power Sources*, **178**(1), pp. 207–222.

[3] Karnik, A., Stefanopoulou, A., and Sun, J., 2007. "Water equilibria and management using a two-volume model of a polymer electrolyte fuel cell". *Journal of Power Sources*, **164**, pp. 590–605.

[4] Love, A., Middleman, S., and Hochberg, A., 1993. "The dynamics of bubblers as vapor delivery systems". *Journal of Crystal Growth*, **129**, pp. 119–133.

[5] Choi, K., Park, D., Rho, Y., Kho, Y., and Lee, T., 1998. "A study of the internal humidification of an integrated pemfc stack". *Journal of Power Sources*, **74**, pp. 146–150.

[6] Staschewski, D., 1996. "Internal humidifying of pem fuel cells". *International Journal of Hydrogen Energy*, **21**(5).

[7] McKay, D., Stefanopoulou, A., and Cook, J., 2008. "Model and experimental validation of a controllable membrane-type humidifier for fuel cell applications". In Proceedings of 2008 American Control Conference, Vol. ACC897.

[8] Wheat, W., Clingerman, B., and Hortop, M., 2005. Electronic by-pass control of gas around the humidifier to the fuel cell. U.S. Patent number 6884534, April.

[9] Cortona, E., Onder, C., and Guzzella, L., 2002. "Engine thermomanagement with electrical components for fuel consumption reduction". *IMechE Int. Journal of Engine Research*, **3**(3), pp. 157–170.

[10] Setlur, P., Wagner, J., Dawson, D., and Marotta, E., 2005. "An advanced engine thermal management system: Nonlinear control and test". *IEEE/ASME Transactions on Mechatronics*, **10**(2).

[11] Khalil, H., 2002. *Nonlinear Systems*. Prentice Hall.

[12] Slotine, J.-J., and Li, W., 1991. *Applied Nonlinear Control*. Prentice-Hall, Inc.

[13] Hang, C., Astrom, K., and Wang, Q., 2002. "Relay feedback auto-tuning of process controllers - a tutorial review". *Journal of Process Control*, **12**(1).

[14] Taylor, J., 1999. "Describing functions". In *Electrical Engineering Encyclopedia*. John Wiley and Sons, Inc., New York.

[15] Middleton, R., and Graebe, S., 1999. "Slow stable open-loop poles: to cancel or not to cancel". *Automatia*, **35**, pp. 877–886.